A COMPARISON OF TIME- AND FREQUENCY-DOMAIN AMPLITUDE MEASUREMENTS

Hans E. Hartse

Los Alamos National Laboratory

Sponsored by National Nuclear Security Administration
Office of Nonproliferation Research and Engineering
Office of Defense Nuclear Nonproliferation

Contract No. W-7405-ENG-36

ABSTRACT

We have been investigating regional body wave detection thresholds and seismic event identification methods. The basis of this research requires accurate phase and noise amplitude measurements, generally involving frequencies of about 1 Hz and higher [for example, P_n/(0.75-1.5 Hz)]. Here, we examine the differences between amplitude measurements made in the time domain and measurements made in the frequency domain and how those differences might affect regional seismic discrimination and detection threshold estimates.

We have worked with WMQ data for several years. We have retrieved and measured seismograms recorded at WMQ from about 1800 events from throughout central Asia for the years ranging from 1986 to 2000. Event-station distances range out to about 2500 km and event magnitudes range from about m_b 2.5 to over 6.0. We measured WMQ BHZ seismograms over the P_n, P_g, S_n, and L_g phases using time domain root mean square (RMS) and frequency domain Fast Fourier Transform (FFT) methods.

For RMS amplitude measurements, we use the instrument response to correct the entire seismogram into displacement. We then bandpass filter, cut the time-window based on velocity and event-station distance, and measure amplitude as a Log_{10} RMS value. For the spectral method, we cut the phase time-window from a seismogram that has been instrument-corrected into acceleration. We then taper, FFT, and divide by angular frequency twice to convert into displacement. We initially instrument-correct the seismogram into acceleration in an effort to reduce the large amplitudes of the longer period microseism relative to the shorter-periods that are of interest to us for discriminant tests. We smooth and resample the spectra at a rate of 0.05 Log_{10} frequency. To compare RMS and spectral amplitudes for a given event, phase, and band we average the displacement spectra over the same band used during the RMS procedure. When comparing the two methods, we convert the RMS amplitudes to pseudo-spectral amplitudes following Parseval's Theorem.

In general, RMS amplitudes of all phases are slightly larger than the corresponding spectral amplitudes. This is because Log_{10} averaging of the spectral amplitudes emphasizes the higher frequencies within a band. These higher frequencies are lower in amplitude because of the "roll-off" in frequency of the seismic source and the greater attenuation at higher frequencies along the seismic path. The actual ratios obtained using the two methods tend to be nearly the same. This is because the small offsets in the RMS amplitudes relative to the spectral amplitudes are about the same for both phases, and the offsets therefore cancel when the RMS ratio is formed.

We found that spectral measurements of short P_n windows (out to event-station distances of about 700 km) are sometimes unusually large compared to the RMS measurements. This occurrence is most pronounced for low-magnitude events when the measurement window is short. Initially we assumed the problem was with our frequency-domain measurements, but we traced this occurrence to a delay introduced by applying a one-pass filter during the time-domain measurement procedure. The delay was moving the P_n energy down the trace and outside of the measurement window. After changing to a two-pass filter, the RMS amplitudes closely matched the spectral amplitudes.

KEY WORDS: phase amplitude, detection, identification

OBJECTIVE

Any phase detection, magnitude estimation, amplitude tomography, or discrimination analysis applied to treaty monitoring situations requires careful, consistent amplitude measurements. To confirm that we are obtaining good estimates of signal and noise, we measured phase and noise amplitudes of regional seismic data using both time-domain and frequency-main methods. As Parseval's Theorem states that frequency-

domain and RMS time-domain measurements are equivalent, our objective is to compare the two methods to confirm that each approach is robust and consistent. Below, we describe our data, processing, and a comparison of our results.

RESEARCH ACCOMPLISHED

At we have worked with station WMQ data for several years. We have retrieved and measured seismograms recorded at WMQ from throughout central Asia for the years ranging from 1986 to 2000. Event-station distances range out to about 2500 km and event magnitudes range from about mb 2.5 to over 6.0. We measured WMQ BHZ seismograms (about 1800 in all) over the P_n, P_g, S_n, and L_g phases using both the time domain and frequency domain methods.

For time-domain processing we pick phase arrivals and then instrument-correct each waveform into units of displacement in meters. The entire seismogram is de-meaned, tapered, and bandpass filtered. Typically, we measure several one-octave (or slightly narrower) bands between 0.5 and 8 Hz. The entire instrument-corrected and bandpass-filtered waveform is saved for data windowing and measurement processes. Phase measurement windows are defined by the velocities in Table 1, and the phase pick time. The phase window length is defined by the "fast" and "slow" velocities and the event-station distance, but the data window is centered over the picked arrival time. If any segment of the waveform record is not available for the time window of interest, then no amplitude measurements are attempted. Hence, for triggered data we will sometimes measure P_n and P_g, but will not be able to measure S_n and L_g. After determining time windows, the filtered seismogram is cut and an RMS amplitude is measured and stored as a Log_{10} value.

Our frequency domain processing is patterned after the Rodgers et al. (1997) processing model. A data window is cut from an instrument-corrected seismogram, an FFT is run, and the spectra are smoothed and evenly sampled over 0.05 log frequency intervals. We cut data and noise windows exactly as described under our time domain processing. Prior to FFT we taper the data (or noise) window, checking and adjusting taper length to ensure the taper does not extend into the phase arrival pick, or the theoretical phase arrival time (if no pick was made). Following FFT, we then write an amplitude spectra file, being careful to save those portions of the spectra that fall within the passband we used during the instrument correction. Further, when working with short time windows, we only save the low-frequency portions of the spectra that are represented by at least 2 cycles within the time window of interest. For instance, for a 4-second-long P_n window, we would only save spectra of 0.5 Hz and greater.

After converting each frequency point along the spectra into a Log_{10} value, we interpolate along the saved spectra at an interval of 0.01 in Log_{10} frequency, We then smooth with a half-width of 5 and then decimate to every fifth log-frequency sample. Hence, we save the smoothed spectra as Log_{10} amplitude values sampled every 0.05 Hz in log frequency. The final spectral range is controlled by the instrument type and the data window length. When working with a particular passband for discrimination, magnitude, or path calibration research, we average over the appropriate spectral samples to obtain a single amplitude value. With the 0.05 Hz in log frequency sampling interval, a one-octave band will be composed of 6 spectral samples that can be averaged to obtain a single amplitude value.

For comparison purposes we convert the RMS amplitudes to pseudo-spectral amplitudes following Parseval's Theorem, and obtain an average spectral value for a given band as described above. We look at the trend and scatter found between the RMS and spectral amplitude populations by plotting each event's RMS amplitude versus its spectral amplitude (such as in Figure 1A), and by plotting the difference between the two methods for each event versus distance (such as Figure 1D).

Figures 1, 2, and 4 compare P_n and S_n RMS amplitudes to spectral amplitudes. The band is 0.75-1.5 Hz. For Figure 1 we applied a four-pole, one-pass Butterworth filter to measure RMS amplitudes, and we estimated spectra from displacement records (following Rodgers et al. (1997). For the P_n results, the spectral amplitudes (Figure 1A) are often much larger than the RMS amplitudes. This same trend is seen in the S_n results (Figure 1B), but the scatter is more limited.

Assuming the scatter of Figure 1 is related to problems with the FFT on short data windows (only 2 to 9 seconds for P_n) in the presence of strong microseism emphasized on the displacement records, we changed our approach to the FFT. We instrument-corrected into acceleration to de-emphasize the longer periods, ran the FFT, and then divided the spectra by angular frequency twice to obtain displacement spectra. Figure 2 shows amplitude results using this modified approach. Scatter is eliminated on the S_n comparison (Figure 2B), and scatter is nearly eliminated on the P_n comparison (Figure 2A). We still find a few P_n spectral amplitudes that are large relative to the RMS amplitudes. This happens when the data window is short [only 2.5 to 5 seconds and event station distances are between about 300 and 500 km (Figure 2C)].

We assumed the remaining P_n scatter was still related to the FFT in the presence of strong microseism despite running the FFT on acceleration records. However, high-pass filtering at 0.5 Hz in an effort to eliminate the microseism prior to FFT did not reduce scatter. Hence, we re-examined our time-domain procedure and found that the four-pole, one-pass Butterworth filter we were applying was introducing a delay that was moving a significant portion of the P_n signal out of the measurement window. The delay is greatest when a narrow filter (relative to the total bandwidth) is applied. Further, the short time window at distances of between 300 and 500 km, combined with an emergent P_n arrival creates a situation where the delay can significantly change the RMS amplitude estimate (Figure 3). We made new RMS measurements using a two-pole, two-pass filter, and nearly eliminated the problem with the P_n scatter (Figure 4). We did not encounter signal-generated noise problems when applying the two-pass filter.

In Figures 1, 2, and 4 the spectral amplitudes were obtained by averaging the Log_{10} values of the spectra. Rodgers et al. (1997) argue that this approach emphasizes the higher frequencies in a given band. To test this idea, we compare the RMS amplitudes to linearly averaged spectra as shown in Figure 5. The Log_{10} averaging reveals a slight trend between the spectral and RMS amplitude differences as distance increases (Figures 4C and 4D). With linear spectra averaging, this trend is only very slightly present (Figures 5C and 5D). Further, scatter is reduced slightly when comparing Figures 5A to 4A and 5B to 4B.

For discrimination, how these measurement methods affect ratios is especially important. Figure 6 compares P_n/S_n ratios for the 0.75-1.5 Hz and the 4-8 Hz bands. The RMS results are obtained using two-pass filters and the spectra have been linearly averaged. The ratios of both bands show good one-to-one trends (Figures 6A and 6B), and the differences between the ratios show almost no trend with distance or measurement window length (Figures 6C and 6D). Log_{10} averaging of the spectra produces nearly the same result.

CONCLUSIONS AND RECOMMENDATIONS

Overall, Figures 4 and 5 show that RMS and spectral measurements are essentially equivalent, and the differences between linear and Log_{10} spectral averaging appear slight. Further, ratios obtained with time-domain measurements are essentially equivalent to ratios obtained with frequency-domain measurements as we expect from Parseval's Theorem. We have now been able to confirm that we have two consistent techniques for measuring regional waveform amplitudes. This investigation did reveal a few signal-processing pitfalls. The FFTs on the short segments of displacement waveforms were apparently contaminated by strong, longer-period microseism. The FFT in acceleration (to enhance the short periods of interest) followed with two divisions by angular frequency corrected the problem. We also uncovered a delay problem with a one-pass filter applied to time-domain data. We corrected this problem by applying a two-pass filter. We did not encounter significant signal-generated noise problems by applying the two-pass filter. When applied with care, we recommend either the time-domain RMS method or the frequency-domain method for regional-phase amplitude measurements.

REFERENCES

Rodgers, A.J., T. Lay, W.R. Walter, and K.M. Mayeda, (1997), A Comparison of Regional-Phase Amplitude Ratio Measurement Techniques, Bull. Seismol. Soc. Am., 87, 1613-1621.

Table 1. Velocities Used For Defining Phase Windows

Phase	V_{ph} $(km\ s^{-1})$	V_{fast} $(km\ s^{-1})$	V_{slow} $(km\ s^{-1})$
P_n	8.10	8.2	7.6
P_g	6.15	6.2	5.2
S_n	4.60	4.7	4.0
L_g	3.50	3.6	3.0

P_n Amplitude Comparisons for 0.75-1.5 Hz Band with FFT in Displacement

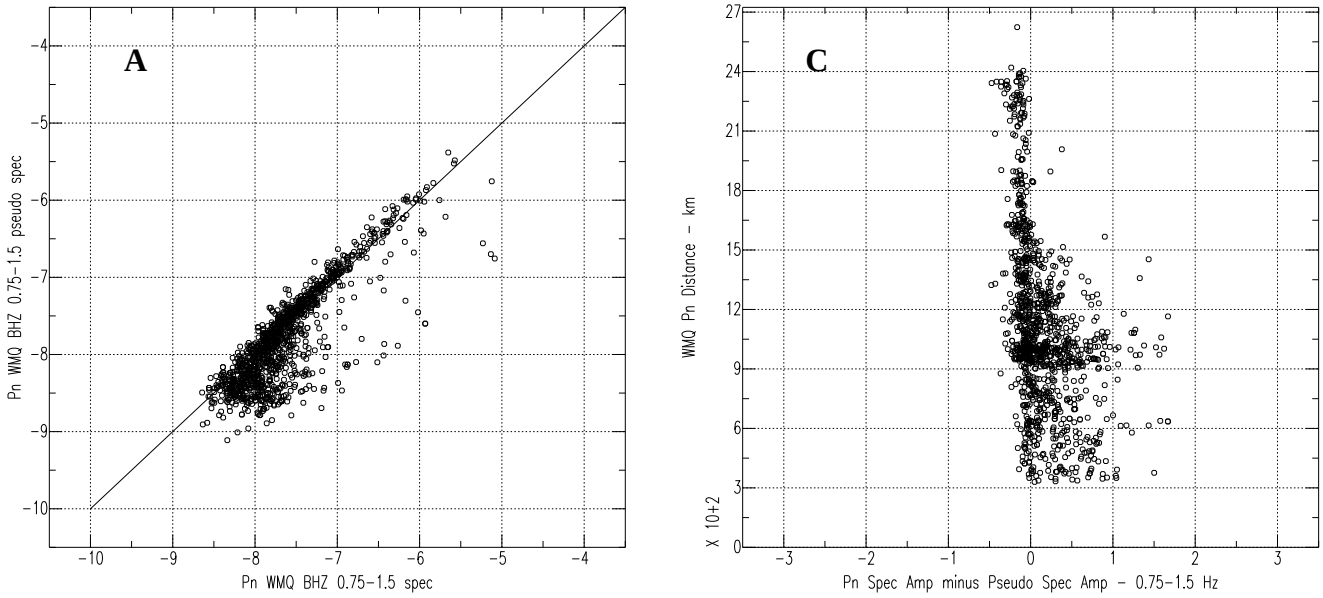

S_n Amplitude Comparisons for 0.75-1.5 Hz Band with FFT in Displacement

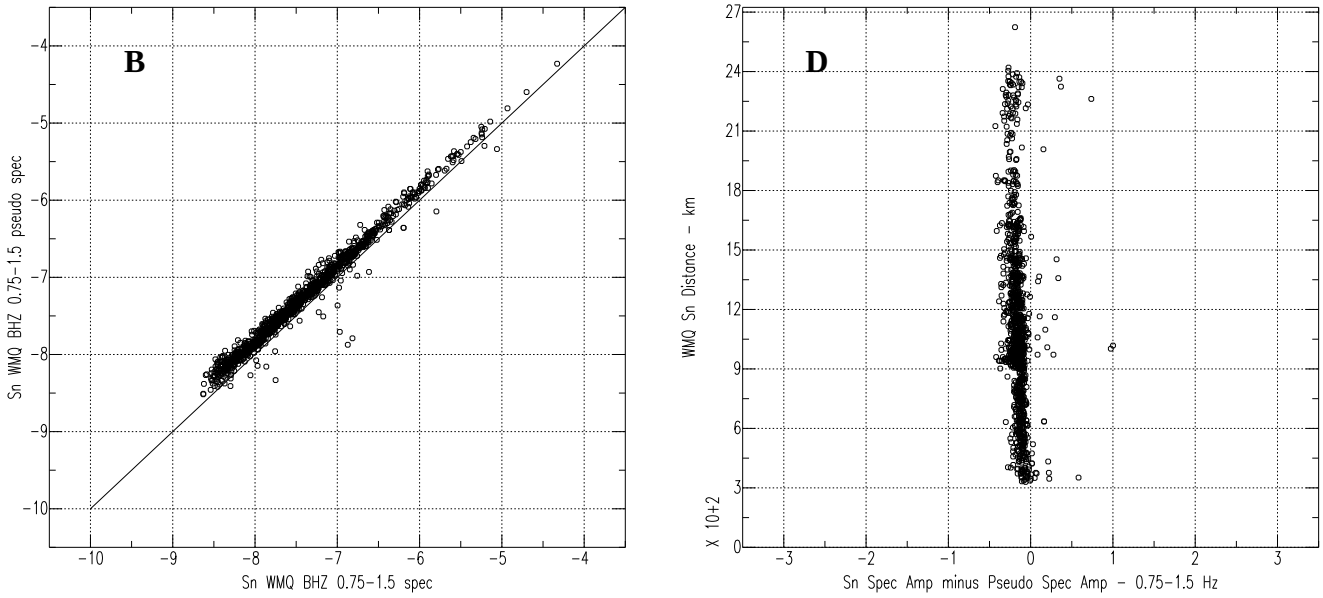

Figure 1. P_n and S_n comparisons between pseudo-spectral amplitudes derived from RMS measurements and spectral amplitudes derived from FFT measurements of displacement seismograms. **A** shows P_n pseudo-spectra (vertical axis) versus P_n spectra estimated directly from displacement waveforms, and **B** shows S_n pseudo-spectra versus S_n spectra estimated directly from displacement waveforms. **C** and **D** show event-station distance on vertical axes versus the difference between spectral and pseudo-spectral amplitudes. Measurement scatter is significant, with many spectral amplitudes much larger than the RMS-derived amplitudes. All measurements are presented in the Log_{10} domain.

P_n Amplitude Comparisons for 0.75-1.5 Hz Band with FFT in Acceleration

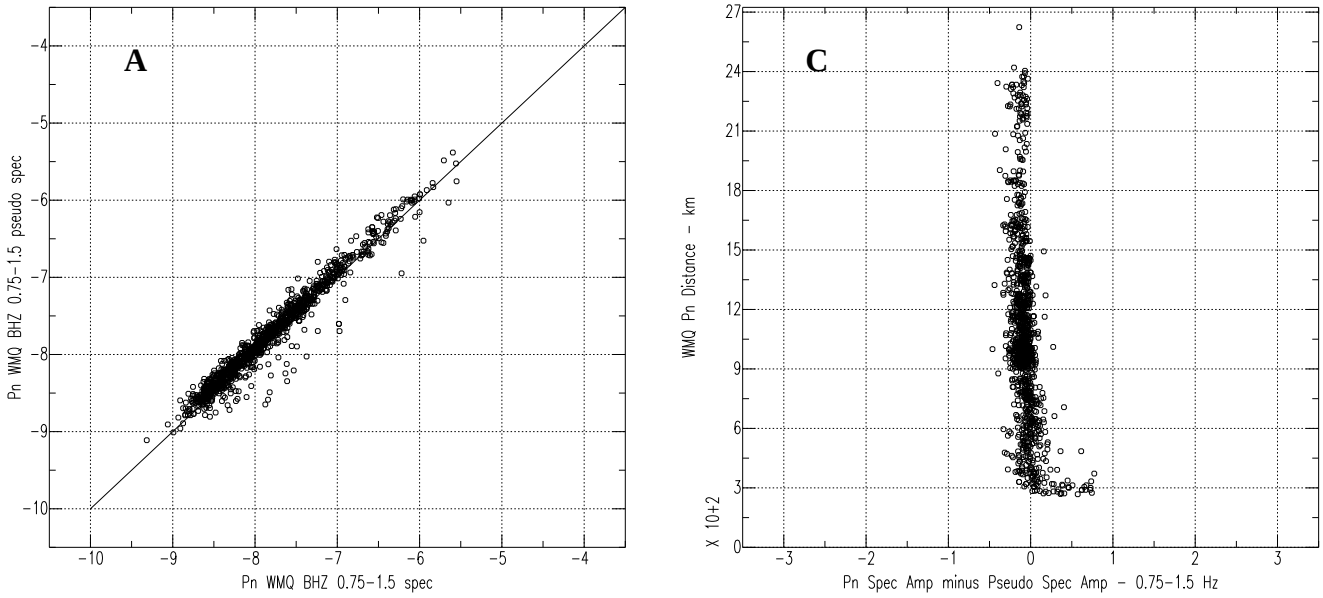

S_n Amplitude Comparisons for 0.75-1.5 Hz Band with FFT in Acceleration

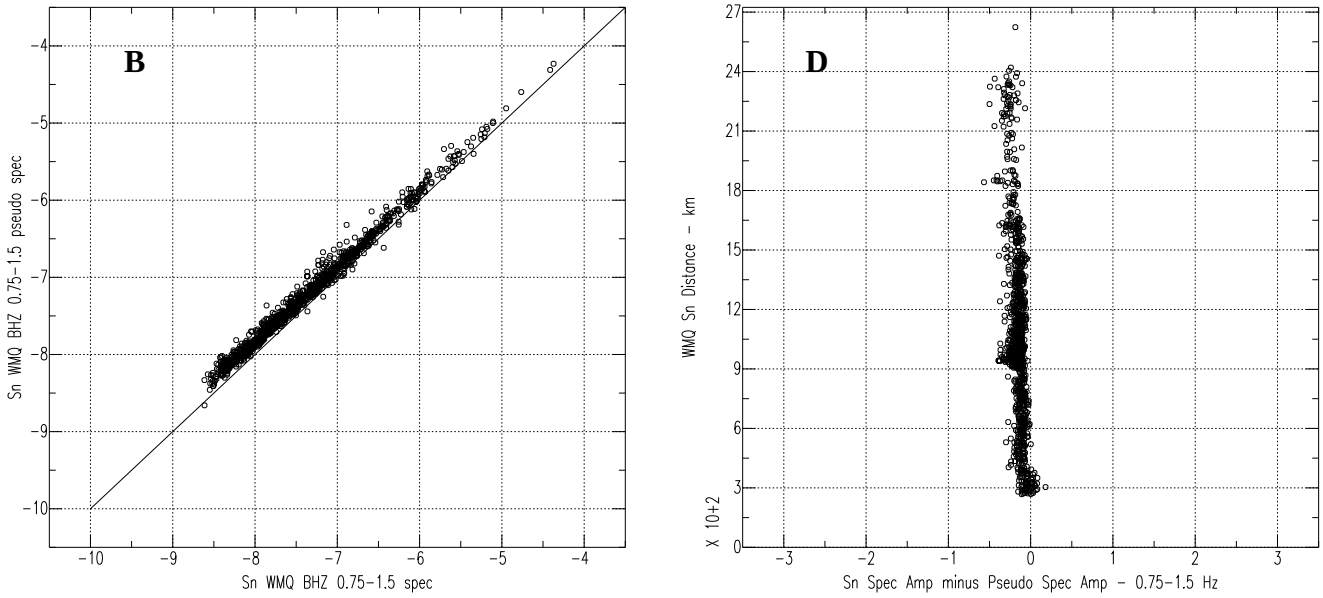

Figure 2. P_n and S_n comparisons between pseudo-spectral amplitudes derived from RMS measurements and spectral amplitudes derived from FFT measurements of acceration seismograms. **A** shows P_n pseudo-spectra (vertical axis) versus P_n spectra estimated from acceleration waveforms division by angular frequency twice to obtain displacement spectra. **B** shows S_n pseudo-spectra versus S_n spectra estimated from acceleration waveforms and division by angular frequency twice. **C** and **D** show event-station distance on vertical axes versus the difference between spectral and pseudo-spectral amplitudes. Measurement scatter is significantly reduced compared to Figure 1 (the case of FFT on displacement waveforms). Some scatter for P_n still remains at short event-station distances between about 300 and 500 km (**A** and **C**).

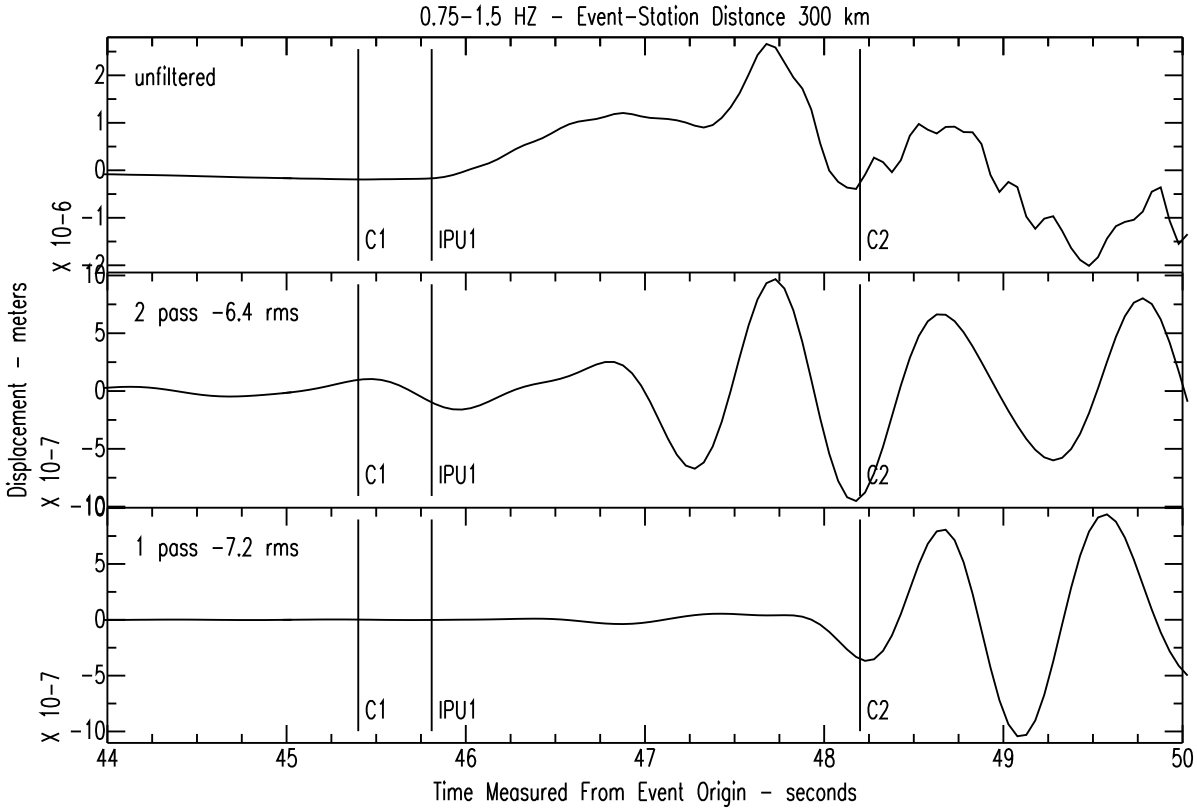

Figure 3. Example where a one-pass 0.75-1.5 Hz Butterworth filter has introduced a delay that pushes the largest P_n amplitudes out of the measurement window, producing an erroneously small RMS amplitude estimate. The top trace is unfiltered, the middle trace has a two-pass 0.75-1.5 Hz filter applied, and the bottom trace has the one-pass filter applied. The C1 and C2 markers indicate the measurement window. Note how the amplitude peak just to the left of C2 on the top and middle traces has been pushed to the right of the C2 marker on the bottom trace. The event-station distance is 300 km, and the event magnitude is 4.7.

P_n Amplitude Comparisons for 0.75-1.5 Hz Band with FFT in Acceleration

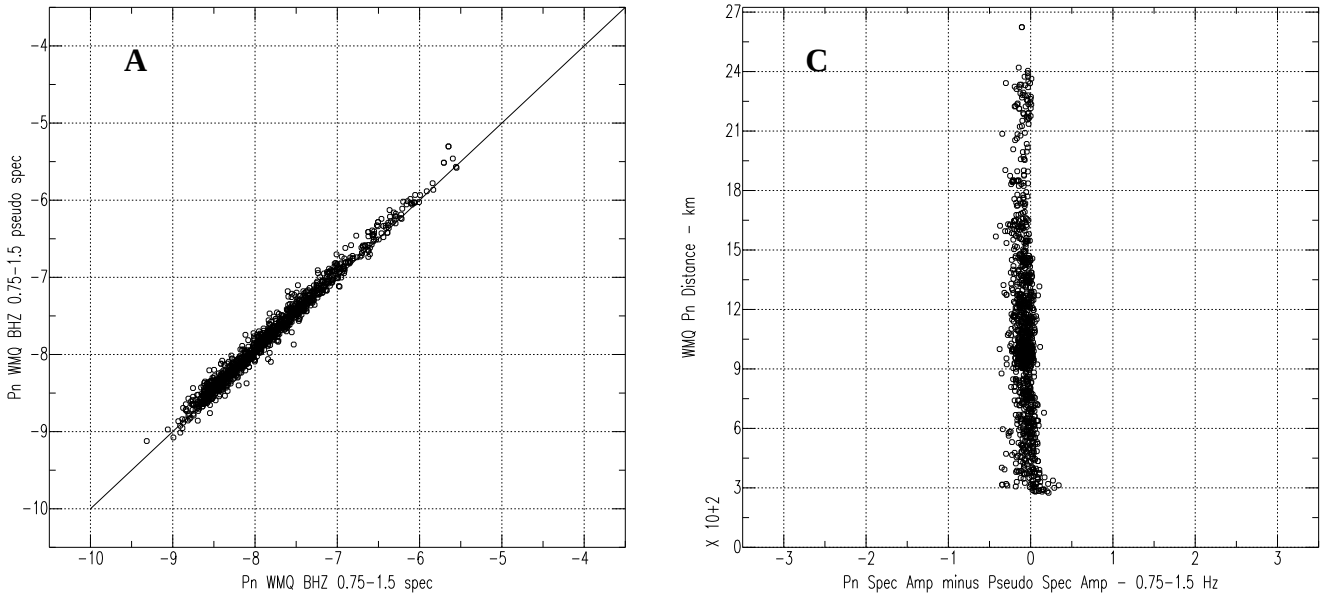

S_n Amplitude Comparisons for 0.75-1.5 Hz Band with FFT in Acceleration

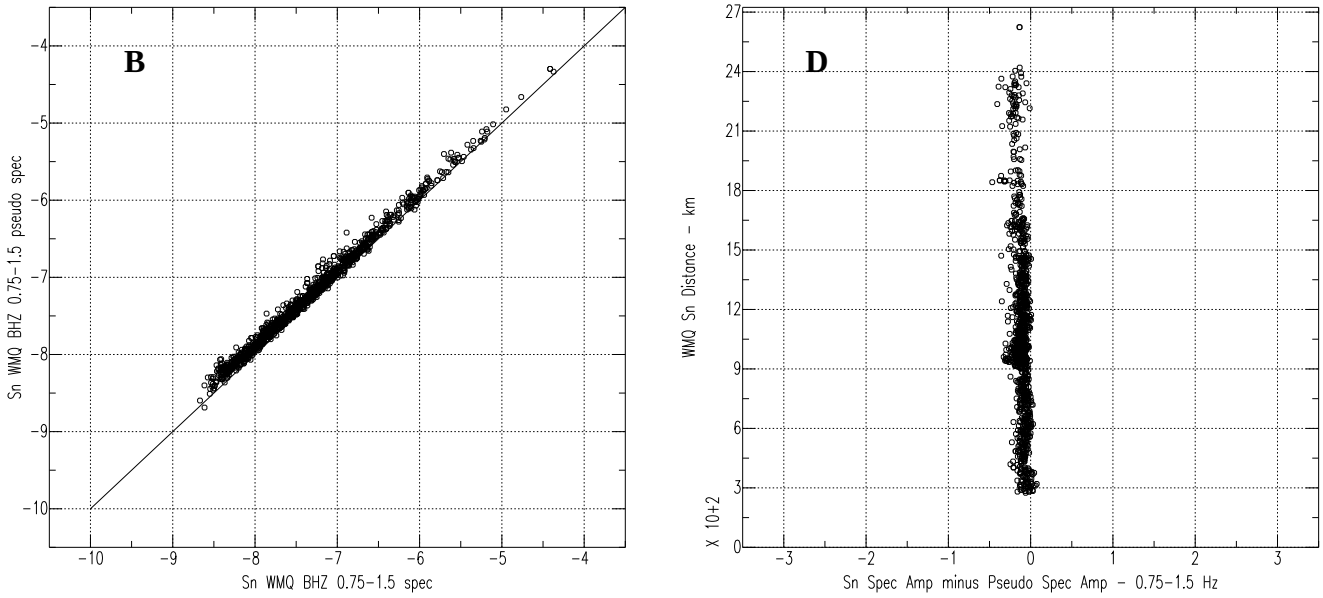

Figure 4. Same as Figure 2, but the time domain measurements have been made with a two-pass filter, rather than a one-pass filter. The delay produced with the one-pass filter had pushed some P_n energy out of the RMS measurement window for the case of event-station distances near 300 km (see Figure 3). Hence, in Figure 2A, the scatter was caused by underestimation of signal strength in the time domain. Here, a two-pass filter has been applied, the delay does not occur, and the P_n scatter has been eliminated. With the longer windows measured for S_n, the scatter is not present (compare Figure 2B with Figure 4B.

P_n Amplitude Comparisons for 0.75-1.5 Hz Band with FFT in Acceleration

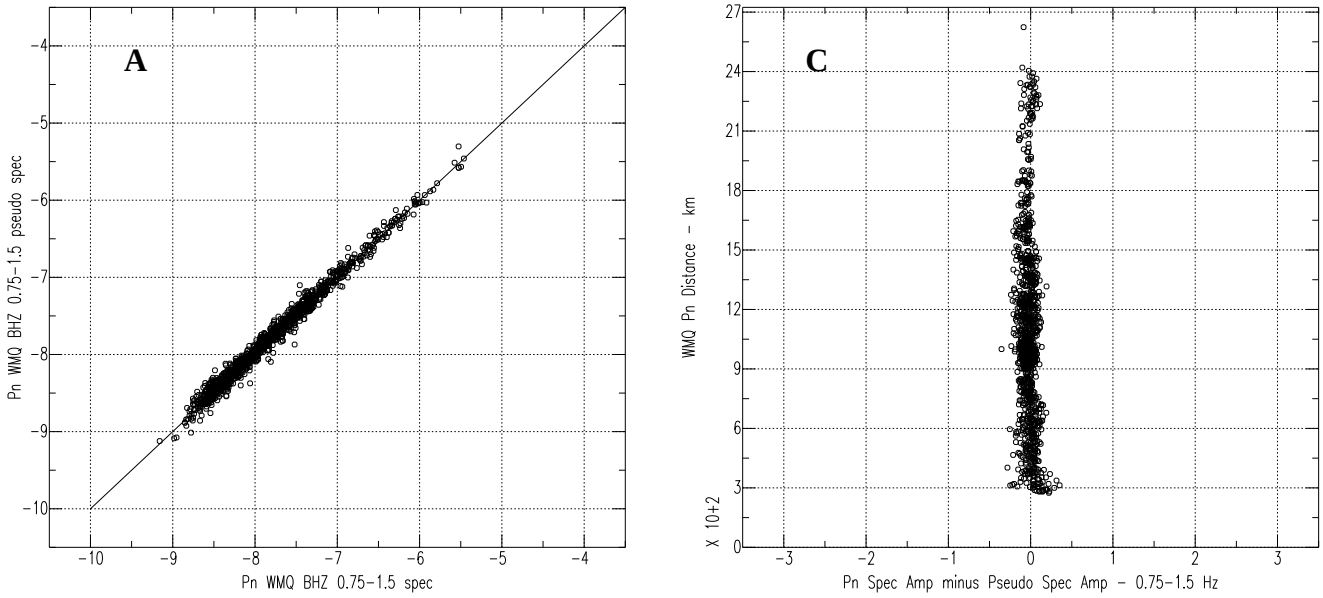

S_n Amplitude Comparisons for 0.75-1.5 Hz Band with FFT in Acceleration

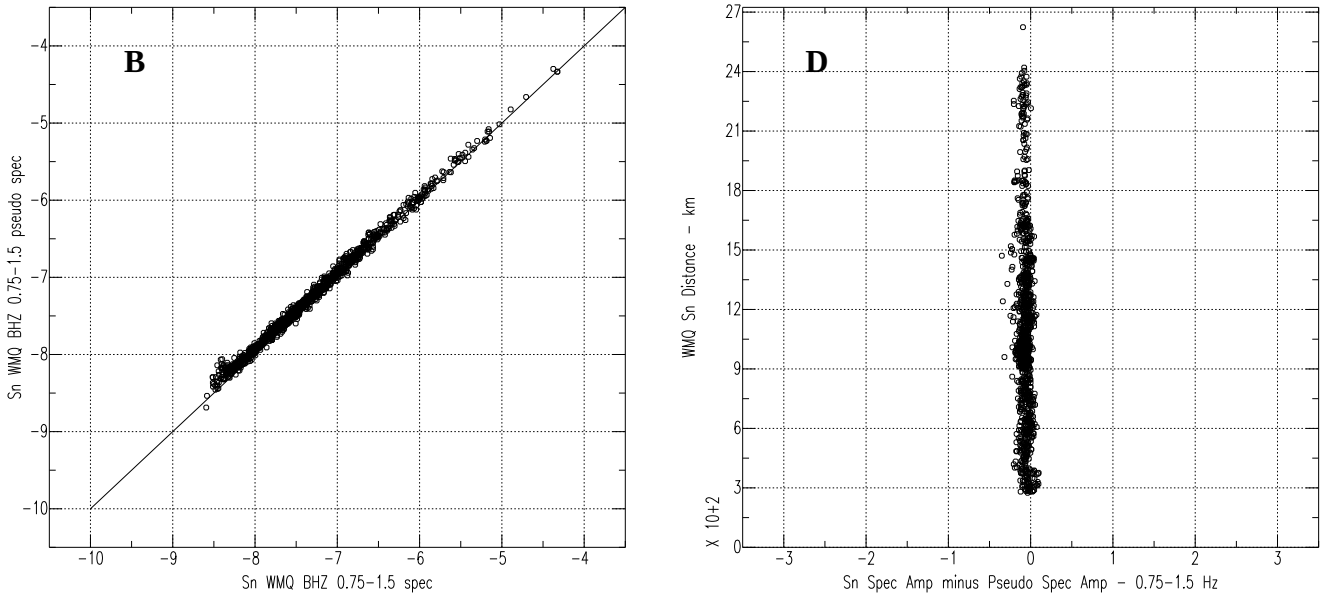

Figure 5. Same as Figure 4, but spectral averaging has been done on linear amplitudes rather than Log_{10} amplitude values. The pseudo-spectra are obtained using a two-pass filter. This is the closest agreement we obtain between spectral and time-domain amplitude measurements.

P_n/S_n Amplitude Ratio Comparisons for 0.75-1.5 Hz Band with FFT in Acceleration

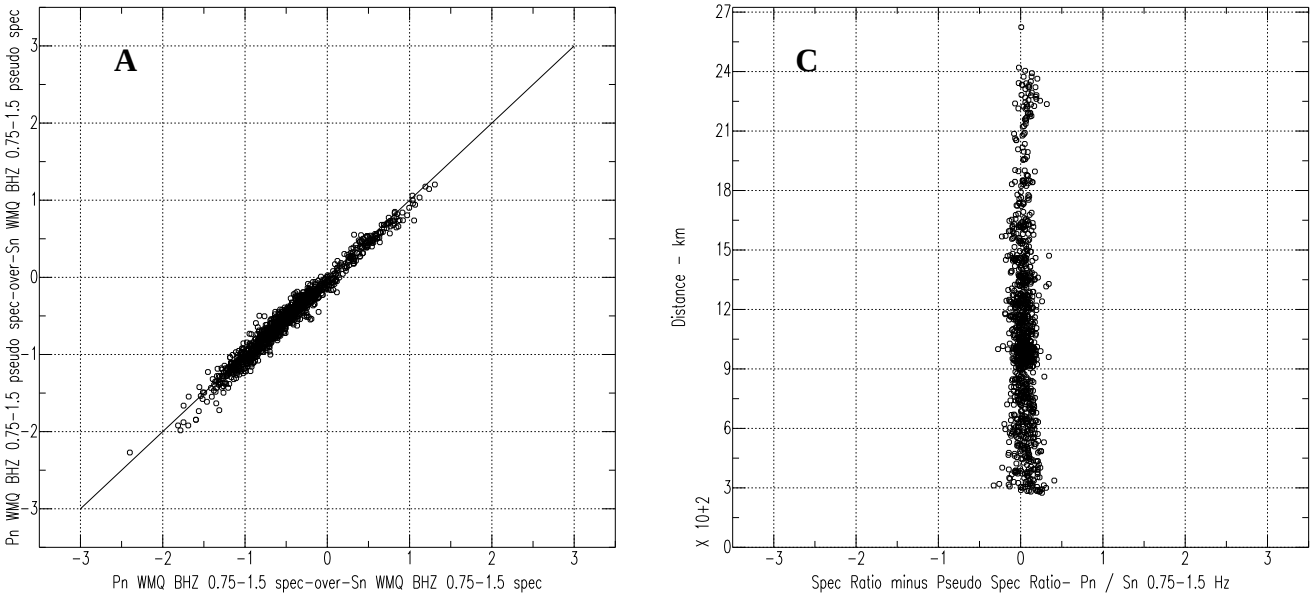

P_n/S_n Amplitude Ratio Comparisons for 4-8 Hz Band with FFT in Acceleration

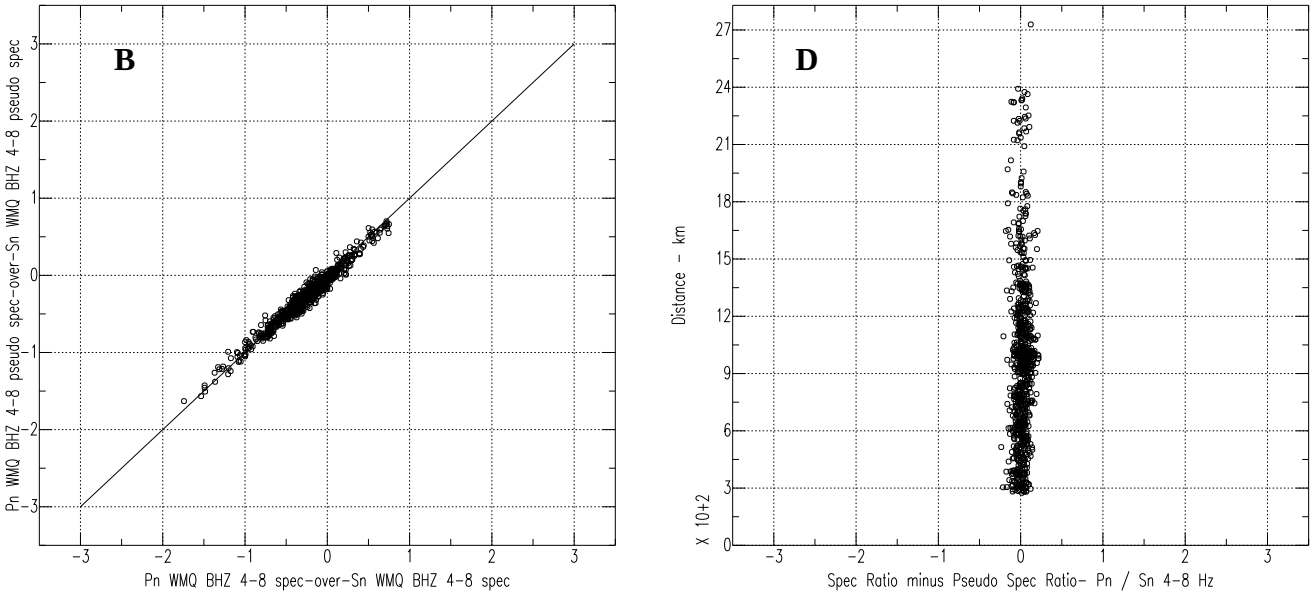

Figure 6. Comparisons of P_n/S_n ratios formed with amplitudes obtained by time-domain and frequency-domain measurements. Linear spectral amplitudes are averaged and pseudo-spectra are obtained using a two-pass filter. For both the 0.75-1.5 Hz and the 4-8 Hz bands the two measurement methods provide very similar results, and only a slight trend with event-station distance can be seen (**C** and **D**). Although not shown here, results obtained through averaging of logrithmic spectral amplitudes are nearly the same.